Letter

5σ tension between *Planck* cosmic microwave background and eBOSS Lyman-alpha forest and constraints on physics beyond ΛCDM

Keir K. Rogers[1,2,*] and Vivian Poulin[3,†]

[1]*Department of Physics, Imperial College London, Blackett Laboratory, Prince Consort Road, London SW7 2AZ, United Kingdom*
[2]*Dunlap Institute for Astronomy and Astrophysics, University of Toronto, 50 St. George Street, Toronto, Ontario M5S 3H4, Canada*
[3]*Laboratoire Univers et Particules de Montpellier (LUPM), Centre National de la Recherche Scientifique (CNRS) et Université de Montpellier, Place Eugène Bataillon, 34095 Montpellier Cédex 05, France*

(Received 4 January 2024; accepted 14 January 2025; published 22 January 2025)

We find that combined *Planck* cosmic microwave background, baryon acoustic oscillations, and supernovae data analyzed under Λ cold dark matter (ΛCDM) are in 4.9σ tension with the extended Baryon Oscillation Spectroscopic Survey (eBOSS) Lyα forest in inference of the linear matter power spectrum at wave number $\sim 1h\,\mathrm{Mpc}^{-1}$ and redshift $= 3$. Model extensions can alleviate this tension: running in the tilt of the primordial power spectrum ($\alpha_s \sim -0.01$); a fraction $\sim(1-5)\%$ of ultralight axion dark matter (DM) with particle mass $\sim 10^{-25}$ eV or warm DM with mass ~ 10 eV. The new Dark Energy Spectroscopic Instrument survey, coupled with high-accuracy modeling, will help distinguish the source of this discrepancy.

DOI: 10.1103/PhysRevResearch.7.L012018

Introduction. The standard models of particle physics and cosmology have been experimentally confirmed with high precision [1,2]. Yet, open questions remain, including the origin of the masses of neutrinos, the source of density fluctuations that evolved into the cosmic large-scale structure (LSS), and the fundamental natures of dark matter (DM) and dark energy (DE).

High-precision datasets such as cosmic microwave background (CMB) temperature T, polarization E,B, and lensing ϕ anisotropies [3–5], baryon acoustic oscillations [BAO; 6] and supernovae magnitudes [SNe; 7] are consistent with the standard Λ cold dark matter (ΛCDM) cosmological model. However, there is disagreement with some other datasets in the inference of cosmological parameters, which is either a sign of unmodeled systematics or deviation from ΛCDM. A local distance ladder using SNe and cepheid stars infers the expansion rate today H_0 to be $\sim 5\sigma$ higher than from an inverse distance ladder using CMB, BAO, and SNe data in the ΛCDM model [8]. Further, some LSS data, in particular, the clustering and lensing of photometric galaxy surveys like the Dark Energy Survey [DES; 9] and the Kilo-Degree Survey [KiDS; 10], show a $2-3\sigma$ preference, compared to CMB, BAO, and SNe data, for a lower value of the cosmological parameter $S_8 \equiv \sqrt{\frac{\Omega_\mathrm{m}}{0.3}}\sigma_8$, where Ω_m is the total matter density and σ_8 is the amplitude of density fluctuations averaged over $8h^{-1}$ Mpc scales today.

CMB data are currently sensitive to the matter power spectrum for wave numbers $k \lesssim 0.2h\,\mathrm{Mpc}^{-1}$ [Fig. 1; see also 4] through the generation of lensing anisotropies. A key probe of physics beyond ΛCDM is therefore the high-k (small scale) matter power spectrum. Indeed, the S_8 discrepancy may be a hint of a small-scale deviation from the standard model, as galaxy clustering and lensing data from DES and KiDS are modeled for $k \lesssim 1h\,\mathrm{Mpc}^{-1}$. Resolutions to the S_8 discrepancy center around scale-dependent changes to the growth of perturbations, e.g., ultralight axion (ULA) DM [11], time-dependent changes, e.g., DM-DE interactions [12–14], decaying DM [15–19], or stronger galactic feedback [20]. However, interpretation is complicated by uncertainties like nonlinearities, the intrinsic alignment of galaxy shapes [21], and a lack of clarity as to the scales at which a discrepancy between CMB and LSS occurs (see below).

The Lyman-α forest, quasar spectral absorption formed in the intergalactic medium (IGM), is a powerful probe of high-k, quasilinear modes for $k \gtrsim 0.3h\,\mathrm{Mpc}^{-1}$ [Fig. 1; see also 22]. This probe therefore provides an independent test of consistency between CMB and LSS data uncomplicated by the problems outlined above, albeit with its own uncertainties regarding the astrophysical state of the IGM. This power arises because it is sourced by moderate IGM fluctuations (tracing underlying DM fluctuations with overdensities $\lesssim 10$) that are much less affected by nonlinearities and galactic feedback than equivalent scales in galaxy surveys [e.g., 23].

The extended Baryon Oscillation Spectroscopic Survey (eBOSS) completed observation of $\sim$200 000 quasar spectra with detectable Lyman-α forest [24]. The high-k power spectrum can be probed by measuring correlations only along the line of sight. The eBOSS Collaboration reports a 1D Lyman-α forest flux power spectrum for velocity wave numbers

*Contact author: k.rogers24@imperial.ac.uk
†Contact author: vivian.poulin@umontpellier.fr

Published by the American Physical Society under the terms of the Creative Commons Attribution 4.0 International license. Further distribution of this work must maintain attribution to the author(s) and the published article's title, journal citation, and DOI.

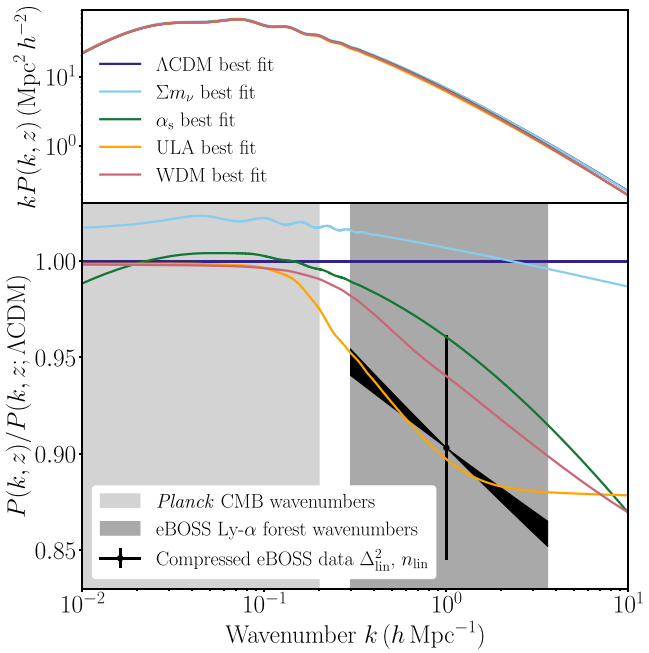


FIG. 1. Best-fit linear matter power spectra at $z = 3$ given *Planck* CMB, BAO, SNe, and eBOSS Lyman-α forest data for the indicated cosmological models. In the bottom panel we show the ratio to the best-fit ΛCDM model. The vertical black error bar indicates the 1σ uncertainty on the amplitude $\Delta^2_{\rm lin}$ of the linear matter power at $z_{\rm p} = 3$, $k_{\rm p} = 0.009\,{\rm s\,km^{-1}} \approx 1h\,{\rm Mpc^{-1}}$ as constrained by eBOSS; the diagonal black band indicates the 1σ uncertainty on the tilt $n_{\rm lin}$. The gray bands show the approximate range of wave numbers to which *Planck* CMB and eBOSS Lyman-α forest are sensitive.

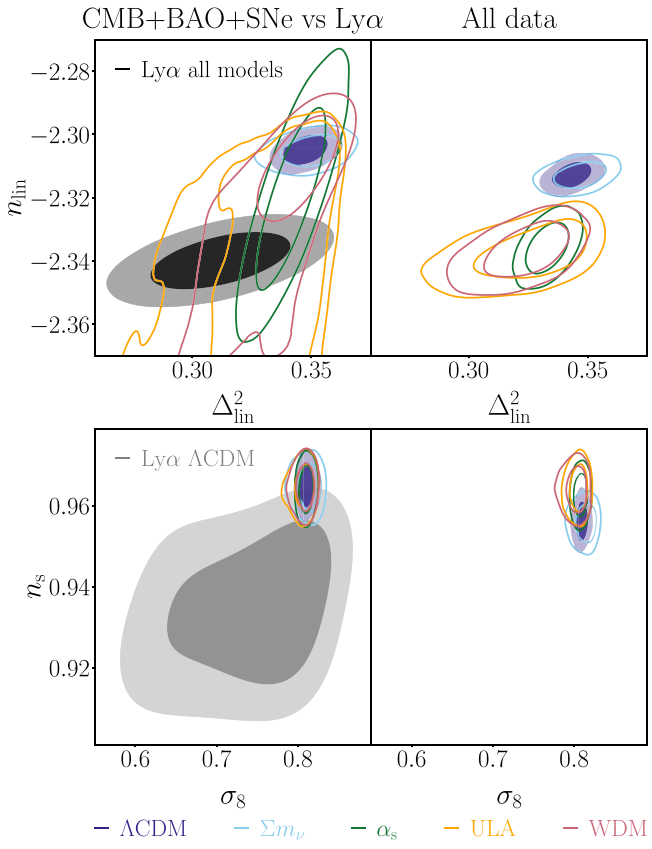


FIG. 2. Marginalized posterior distributions of $\Delta^2_{\rm lin}, n_{\rm lin}, \sigma_8, n_{\rm s}$ given *Planck* CMB + BAO + SNe (left panels, colored contours), eBOSS Lyman-α forest only (Lyα; left panels, black and gray contours) and the combination of all data (right panels) and the cosmological models indicated by the corresponding color. We show the 68% and 95% credible regions. For the top-left panel, the Lyα forest constraint is the same for all models.

$0.001\,{\rm s\,km^{-1}} < k_{\rm F} < 0.02\,{\rm s\,km^{-1}}$ (approximately equating to the spatial wave numbers shaded in Fig. 1) for redshifts $2.1 < z < 4.7$ [25]. Analyzing the data with a suite of IGM hydrodynamical simulations [26], they constrain ΛCDM parameters σ_8, $\Omega_{\rm m}$ and the tilt of the primordial power spectrum $n_{\rm s}$. They find no significant cosmological parameter tension with CMB data [25,27].

In this work we show that the apparent agreement between datasets arises from considering only standard ΛCDM parameters. Using a compressed likelihood that captures all the information contained in the data for the cosmological models that we consider, we assess consistency at the scales and redshifts to which eBOSS data are sensitive, measuring a $\sim 5\sigma$ discrepancy with CMB, BAO, and SNe data. We then carry out the first analysis of the eBOSS flux power spectrum for a number of extended cosmological models, finding that they alleviate the tension.

Data likelihoods. For a number of cosmological models (ΛCDM, massive neutrinos, power spectrum running, spatial curvature), all the cosmological information in the eBOSS flux power spectrum can be compressed to the amplitude ($\Delta^2_{\rm lin} \equiv \frac{k_{\rm p}^3 P_{\rm lin}(k_{\rm p},z_{\rm p})}{2\pi^2}$) and tilt ($n_{\rm lin} \equiv \frac{{\rm d}\ln P_{\rm lin}(k,z)}{{\rm d}\ln k}|_{k_{\rm p},z_{\rm p}}$) of the linear matter power spectrum $P_{\rm lin}(k,z)$ evaluated at a central redshift $z_{\rm p} = 3$ and wave number $k_{\rm p} = 0.009\,{\rm s\,km^{-1}}$. This compression holds for models that are sufficiently close to Einstein–de Sitter expansion for the redshifts probed by data and where the linear matter power spectrum is well approximated by a power-law relation for the wave numbers probed by data [28–31]. Further, when combining with external CMB data, it is accurate to use the marginal likelihood on $\Delta^2_{\rm lin}, n_{\rm lin}$ [30]. In the Supplemental Material [32], we confirm that the compression holds for mixed ULA and warm dark matter (WDM) models. We therefore use a compressed 2D Gaussian likelihood derived from the eBOSS (Sloan Digital Sky Survey Data Release 14; SDSS DR14) Lyman-α forest flux power spectrum [25] and tabulated in Ref. [33]:[1] the mean values of $\Delta^2_{\rm lin}$ and $n_{\rm lin}$ are respectively 0.310 and -2.340, the standard deviations are respectively 0.020 and 0.006 and the correlation coefficient is 0.512 (Fig. 2). We give de-

[1]The likelihood of Ref. [25] is not publicly available and so Ref. [33] tabulated it (in their Table I) by fitting a 2D Gaussian to a 30×30 grid of likelihood samples from Fig. 20 of Ref. [25]. There is a slight non-Gaussian feature that is not captured, but if the full likelihood were available, we do not anticipate that our conclusions would change. Further, Ref. [27] extends the analysis of Ref. [25] by testing extended cosmological models, but the data and likelihood are the same in both analyses; the astrophysical priors are different in the two analyses.

tails in the Supplemental Material [32] on the astrophysical model which is marginalized. We also sometimes use a compendium of *Planck* 2018 CMB [1,3], galaxy BAO [34–36], and Pantheon+ SNe [7] data that constitutes a larger-scale complement to the smaller scales probed by the eBOSS flux power spectrum; full details are given in the Supplemental Material [32].

Models and inference. We consider four extensions to the baseline six-parameter ΛCDM model: (i) varying the sum of neutrino masses Σm_ν; (ii) the running of the primordial spectral index $\alpha_s \equiv \frac{dn_s}{d\ln k}$; (iii) ultralight axions with particle mass $m_{\rm ULA}$ forming a fraction $f_{\rm ULA}$ of the DM; (iv) warm dark matter with particle mass $m_{\rm WDM}$ and temperature $T_{\rm WDM}$ (forming a fraction $f_{\rm WDM}$ of the DM). The linear matter power spectrum and other cosmological background observables are calculated for these models using the Einstein-Boltzmann solver AXICLASS [37,38]. We use a uniform prior on Σm_ν, α_s, $\log[m_{\rm ULA}]$, $f_{\rm ULA}$, $\log[m_{\rm WDM}]$, $T_{\rm WDM}$, and the standard ΛCDM parameters. We restrict the ULA and WDM fractions to be no greater than 0.05 to ensure that we satisfy the condition for using the compressed likelihood while still optimizing the joint fit to CMB and Lyman-α forest data. More details are given on the models, prior and posterior sampling method in the Supplemental Material [32]. The neutrino and running models are constrained by eBOSS Lyman-α forest data in Ref. [27], to which we compare our results below.

Results. Figure 2 shows the marginalized posterior of $\Delta^2_{\rm lin}, n_{\rm lin}, \sigma_8, n_s$. For the models that we consider, all the cosmological information in the eBOSS Lyman-α forest is contained in $\Delta^2_{\rm lin}, n_{\rm lin}$ and so the posterior of those parameters is the same for each model. When the information in the flux power spectrum is projected to σ_8, n_s, which characterize the amplitude and tilt of the linear matter power spectrum at different redshifts and smaller wave numbers, the relative constraint on these parameters is weaker than for $\Delta^2_{\rm lin}, n_{\rm lin}$. As a consequence, there is broad agreement between CMB + BAO + SNe and Lyman-α forest data when considering only those parameters, even under the ΛCDM model. In the Supplemental Material, we explore the use of prior information, in particular on H_0, in order to set the conversion from native velocity to spatial wave numbers but still find broad consistency with CMB + BAO + SNe. However, when projecting the information in *Planck*, BAO, and SNe data to the larger pivot wave number that eBOSS probes there is a 4.90σ tension[2] under ΛCDM (Table I) driven by a suppressed small-scale power spectrum amplitude and tilt. This tension is not alleviated when varying neutrino masses, since the suppression is steplike at the wave numbers to which eBOSS is sensitive (Fig. 1). However, the tension is reduced to 0.92σ, 1.34σ, and 0.56σ, respectively, for the one-parameter power spectrum running and two-parameter WDM and ULA models; these models suppress both power amplitude and spectral index.

For completeness, we show joint posteriors under all the models we consider (right panels of Fig. 2 with parameter constraints and $\Delta\chi^2$ given in Table I and the Supplemental Material [32]); however, the ΛCDM and neutrino constraints are unreliable, as the CMB and Lyman-α forest data remain in $\sim 5\sigma$ tension under these models. The running, ULA, and WDM models are able to recover lower values of $n_{\rm lin}$, $\Delta^2_{\rm lin}$ that eBOSS favors, while maintaining n_s, σ_8 consistency with *Planck*. The physics driving these results is elucidated by the minimum-likelihood (best-fit) linear matter power spectra in Fig. 1. Increasing the mass of neutrinos causes a steplike suppression relative to ΛCDM; in attempting to fit the small-scale tilt, the neutrino masses are set too low to cause sufficient suppression. The best improvements in the total χ^2 arise from the running, ULA, and WDM models. Figure 3 shows joint posteriors of extended model parameters (full sets of 1D and 2D marginalized posteriors in the Supplemental Material). Increasing neutrino masses marginally suppress the small-scale amplitude but cannot lower the small-scale tilt sufficiently. Increasing the deviation from no running can successfully lower the small-scale amplitude and tilt, in agreement with Ref. [27] (see Supplemental Material for results where we simultaneously vary Σm_ν and α_s). The ULA constraint, which disfavors the case with no axions, has a characteristic "w" shape. The WDM constraint shows an anticorrelation between particle mass and temperature with marginalized limits $\log[m_{\rm WDM}\,({\rm eV})] = 1.01\pm^{0.30}_{0.44}$ and $\frac{T_{\rm WDM}}{T_{\rm CMB}} = 0.194\pm^{0.043}_{0.074}$, where $T_{\rm CMB}$ is the CMB temperature, giving $f_{\rm WDM} = 0.0219\pm^{0.0030}_{0.0042}$ (all mean and 68% c.l.). For both ULA and WDM, as the particle mass increases, the suppression wave number increases until it is larger than the eBOSS pivot and so does not lower $\Delta^2_{\rm lin}$. For a given mass, there is a range of ULA fractions and WDM temperatures that moves the power spectrum transfer function to have the correct amplitude and tilt.

Discussion and conclusions. We show that while eBOSS and *Planck* show broad consistency in inference on σ_8, n_s, they are in 4.9σ tension in $\Delta^2_{\rm lin}, n_{\rm lin}$ under the ΛCDM model. This result arises since eBOSS probes wave numbers ($k \sim$

TABLE I. *From left to right*, the parameter tension under the model indicated in the leftmost column between *Planck* CMB + BAO + SNe and eBOSS Lyman-α forest data; the change in the χ-square $\Delta\chi^2$ for the combined dataset relative to ΛCDM; and 1D marginalized posterior mean and 68% credible limits on extended model parameters (95% upper limits on Σm_ν and $m_{\rm WDM}$). Although for completeness we quote marginalized summaries for all extended models, for the neutrino model there remains tension and so constraints are unreliable. Further, the ULA and WDM posteriors are highly non-Gaussian (Fig. 3), so summary statistics must be understood in that context.

Model	Tension (σ)	$\Delta\chi^2$	Parameter constraints
ΛCDM	4.90	–	–
Σm_ν	4.80	−1.9	$\Sigma m_\nu < 0.110\,{\rm eV}$
$\alpha_s \equiv \frac{dn_s}{d\ln k}$	0.92	–25.61	$\alpha_s = -0.0108 \pm 0.0022$
ULA	0.56	–27.58	$\log[m_{\rm ULA}({\rm eV})] = -24.9\pm^{1.5}_{1.1}$
			$f_{\rm ULA} = 0.0146\pm^{0.0014}_{0.0086}$
WDM	1.34	–27.08	$\log[m_{\rm WDM}({\rm eV})] = 1.01\pm^{0.30}_{0.44}$
			$f_{\rm WDM} = 0.0219\pm^{0.0030}_{0.0042}$

[2]We measure tension in the non-Gaussian marginalized $\Delta^2_{\rm lin}, n_{\rm lin}$ constraints using the parameter difference posterior distribution as implemented in the TENSIOMETER package [39].

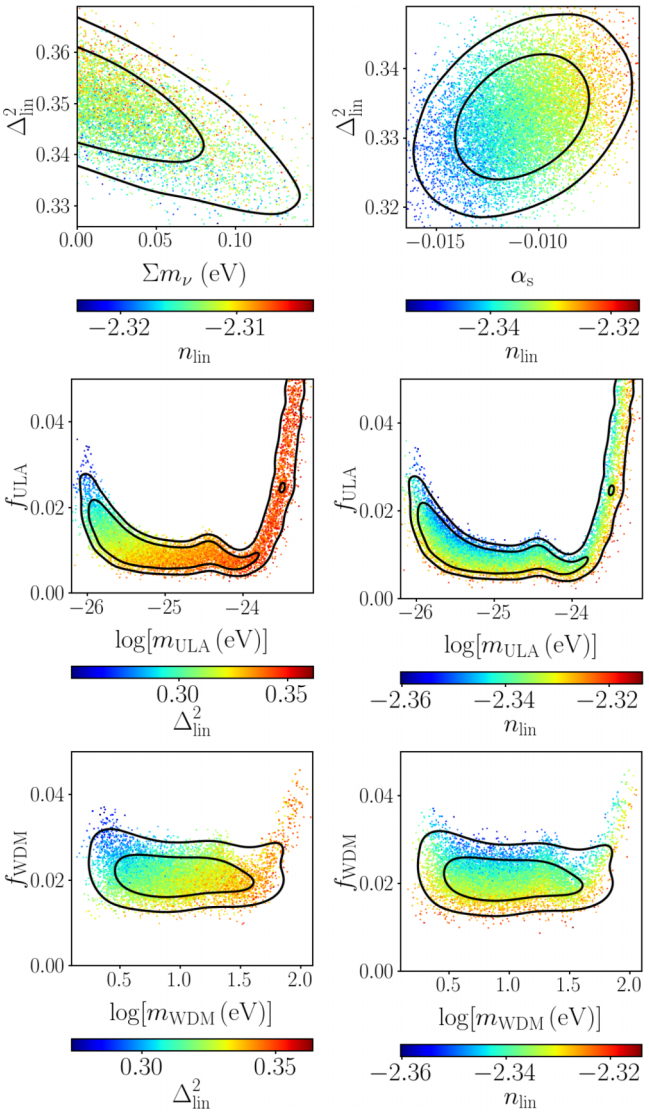


FIG. 3. Marginalized posterior distributions of extended cosmological model parameters and $\Delta^2_{\rm lin}$, $n_{\rm lin}$ given *Planck* CMB + BAO + SNe + eBOSS Lyman-α forest. We show the 2D 68% and 95% credible regions and indicate dependence on a third parameter by the color.

$1\,h\,{\rm Mpc}^{-1}$) larger than those to which σ_8 ($k \sim 0.25\,h\,{\rm Mpc}^{-1}$) and $n_{\rm s}$ ($k \sim 0.07\,h\,{\rm Mpc}^{-1}$) are sensitive, while also being unable, without external information, to constrain simultaneously all ΛCDM parameters. When the eBOSS constraint on $\Delta^2_{\rm lin}, n_{\rm lin}$ is projected to $\sigma_8, n_{\rm s}$, it weakens, whereas the CMB + BAO + SNe constraint on ΛCDM is sufficiently strong that it cannot accommodate the suppressed small-scale matter power spectrum amplitude and tilt that eBOSS measures. We conclude that it is crucial to assess consistency between datasets at the wave numbers and redshifts to which data are sensitive; otherwise, inconsistency can be missed.

We find that varying the masses of neutrinos cannot resolve this parameter discrepancy. This means that constraints on neutrino masses (when not varying any additional parameters) from *Planck* CMB and eBOSS Lyman-α forest are derived from datasets in significant tension and therefore may not be reliable; Ref. [27] presents limits when varying neutrino and running parameters (see also Supplemental Material [32]).[3] We set the first constraints on the ULA and WDM fractions from eBOSS Lyman-α forest; we find a preference for ULAs with $m_{\rm ULA} \sim 10^{-25}$ eV and $f_{\rm ULA} \sim (1-5)\%$ improving the best fit by $\Delta\chi^2 = -27.6$ over ΛCDM with no residual tension (0.56σ). Similarly, we find a contribution of WDM improves the fit by $\Delta\chi^2 = -27.1$ with $m_{\rm WDM} \sim 10$ eV, $T_{\rm WDM} \simeq 0.19\,T_{\rm CMB}$, and reduced tension ($1.34\sigma$). With one fewer free parameter, running of the power spectrum reduces the tension to 0.92σ and improves the fit by $\Delta\chi^2 = -25.6$ [see also 27].

A key effect that changes the tilt of the matter power spectrum inferred from the Lyman-α forest is residual contamination from high-column-density (HCD) absorbers [25–27]. The eBOSS Collaboration found that using a more accurate model for residual HCDs [40,41], calibrated on *Illustris* hydrodynamical simulations [42,43], does not improve the flux power spectrum fit. However, there are other systematic effects related to HCDs that are ignored in 1D Lyman-α forest analyses but which our results suggest should now be investigated, e.g., the masking of HCDs in data is correlated to the large-scale structure; the efficiency of detection and masking is uncertain and so the residual population is unknown. Further, Ref. [44] demonstrated that mismodeling of baryonic feedback from active galactic nuclei (AGN) can bias inference on $n_{\rm s}$ by $\sim 2\sigma$ using the Horizon-AGN simulations [45]. Given that the S_8 discrepancy can be explained by extremely strong feedback models [20], coupled with our new results, it is timely to consider the effect of feedback given different (more physical) hydrodynamical models, e.g., FIRE [46].

Reference [47] reanalyzed the eBOSS flux power spectrum with simulations including spatial fluctuations in helium reionization [48], finding a higher value of the power spectrum tilt that would disfavor running models relative to ULAs, although their astrophysical model is not completely consistent between flux power spectrum and high-resolution spectrum IGM temperature [49] measurements.[4] Reference [50] also reanalyzed the data, finding a higher value of the tilt, albeit with a strong sensitivity in their inference to the prior distribution on the mean transmitted flux. Reference [33] performed ΛCDM and early dark energy analyses using the compressed eBOSS likelihood; we use the compression as tabulated by Ref. [33] and therefore find our ΛCDM constraints are the same. For upcoming Dark Energy Spectroscopic Instrument (DESI) data [51], where the statistical precision will reach percent level, it is crucial that the fidelity of IGM simulations further increases, accounting for scale-dependent effects like HCDs. Coupled with higher-accuracy IGM simulations, it will be feasible to distinguish further between the models we have analyzed and astrophysical uncertainties like HCDs. LSS measurements of the matter power spectrum, e.g., at the Rubin Observatory [52] and Simons Observatory [53], will be highly complementary.

[3]Indeed, this inconsistency applies for any model that does not induce suppression and runs on small scales.

[4]This inconsistency may be relieved by varying cosmology when fitting the high-resolution data [S. Bird, private communication].

Models that reduce the eBOSS Lyman-α forest tension suppress power at higher wave numbers, $k \sim 10\,h\,\mathrm{Mpc}^{-1}$, that are probed by, e.g., higher-resolution Lyman-α forest [54–61] and Milky Way substructure [62–64]. We anticipate that the $\sim$10% suppression implied by eBOSS is consistent at the current sensitivity of higher-resolution flux power spectrum measurements from *Keck* and VLT (which have $\sim$25% uncertainty); the XQ-100 Lyman-α forest dataset [58], which probes smaller scales than eBOSS, infers an even lower value of n_{lin}, which may favor power spectrum running models.[5] Hints of new physics were found in the HIRES/MIKE quasar sample [65,66]. Reference [67] identified a $\sim 3.3\sigma$ discrepancy in the inference of σ_8 between XQ-100 and the HIRES/MIKE Lyman-α forest and galaxy cluster number counts from the South Pole Telescope Sunyaev-Zel'dovich effect [68]; they discuss HCD contamination in the context of this tension. We defer a detailed joint analysis of eBOSS and small-scale structure probes to future work.

Finally, we find in our joint analyses that no model recovers low enough σ_8 to restore consistency with the ΛCDM values inferred from galaxy weak lensing (see Fig. 2 and the Supplemental Material [32] for more details). However, the same argument for the Lyman-α forest applies to weak lensing; we must assess consistency at the scales and redshifts to which weak lensing probes are sensitive. Our work demonstrates that it is critical to use model parametrizations that capture the information content of a given experiment; we present a concrete step in this direction.

Acknowledgments. The authors thank Simeon Bird, Andreu Font-Ribera, Julien Lesgourgues, Riccardo Murgia, and Nils Schöneberg for valuable comments. The authors also thank Cosmology Talks mini-workshops where elements of this project were conceived. K.K.R. is supported by an Ernest Rutherford Fellowship from the UKRI Science and Technology Facilities Council (Grant No. ST/Z510191/1). The Dunlap Institute is funded through an endowment established by the David Dunlap family and the University of Toronto. V.P. is supported by funding from the European Research Council (ERC) under the European Union's HORIZON-ERC-2022 (Grant Agreement No. 101076865). V.P. is also supported by the European Union's Horizon 2020 Research and Innovation program under Marie Skłodowska-Curie Grant Agreement No. 860881-HIDDeN. The authors acknowledge the use of computational resources from the Excellence Initiative of Aix-Marseille University (A*MIDEX) of the Investissements d'Avenir program and from the LUPM's cloud computing infrastructure founded by Ocevu Labex and France-Grilles.

[5]We do not use the compressed XQ-100 likelihood [33] as it has been compressed at the eBOSS pivot wave number, despite XQ-100 data being sensitive to smaller scales. This approach necessarily means that a power-law matter power spectrum model has been assumed from eBOSS to XQ-100 scales, which does not apply to the extended cosmological models that we consider. We defer to future work a detailed analysis with dedicated simulations.

[1] N. Aghanim *et al.* (Planck Collaboration), Planck 2018 results. VI. Cosmological parameters, Astron. Astrophys. **641**, A6 (2020), [Erratum: Astron. Astrophys. **652**, C4 (2021)].

[2] R. L. Workman and Others (Particle Data Group), Review of particle physics, Prog. Theor. Exp. Phys. **2022**, 083C01 (2022).

[3] N. Aghanim *et al.* (Planck Collaboration), Planck 2018 results, V. CMB power spectra and likelihoods, Astron. Astrophys. **641**, A5 (2020).

[4] M. S. Madhavacheril *et al.* (ACT Collaboration), The atacama cosmology telescope: DR6 gravitational lensing map and cosmological parameters, Astrophys. J. **962**, 113 (2024).

[5] L. Balkenhol, D. Dutcher, A. Spurio Mancini, A. Doussot, K. Benabed, S. Galli, P. A. R. Ade, A. J. Anderson, B. Ansarinejad, M. Archipley, A. N. Bender, B. A. Benson, F. Bianchini, L. E. Bleem, F. R. Bouchet, L. Bryant, E. Camphuis, J. E. Carlstrom, T. W. Cecil, C. L. Chang *et al.* (SPT-3G Collaboration), Measurement of the CMB temperature power spectrum and constraints on cosmology from the SPT-3G 2018 TT, TE, and EE dataset, Phys. Rev. D **108**, 023510 (2023).

[6] J. E. Bautista *et al.*, The Completed SDSS-IV extended Baryon Oscillation Spectroscopic Survey: measurement of the BAO and growth rate of structure of the luminous red galaxy sample from the anisotropic correlation function between redshifts 0.6 and 1, Mon. Not. R. Astron. Soc. **500**, 736 (2020).

[7] D. Brout *et al.*, The Pantheon+ analysis: Cosmological constraints, Astrophys. J. **938**, 110 (2022).

[8] A. G. Riess *et al.*, A comprehensive measurement of the local value of the Hubble constant with 1 km s^{-1} Mpc^{-1} uncertainty from the Hubble Space Telescope and the SHOES Team, Astrophys. J. Lett. **934**, L7 (2022).

[9] T. M. C. Abbott *et al.* (DES Collaboration), Dark Energy Survey Year 3 results: Cosmological constraints from galaxy clustering and weak lensing, Phys. Rev. D **105**, 023520 (2022).

[10] C. Heymans *et al.*, KiDS-1000 Cosmology: Multi-probe weak gravitational lensing and spectroscopic galaxy clustering constraints, Astron. Astrophys. **646**, A140 (2021).

[11] K. K. Rogers, R. Hložek, A. Laguë, M. M. Ivanov, O. H. E. Philcox, G. Cabass, K. Akitsu, and D. J. E. Marsh, Ultra-light axions and the S_8 tension: Joint constraints from the cosmic microwave background and galaxy clustering, J. Cosmol. Astropart. Phys. 06 (2023) 023.

[12] R. Murgia, S. Gariazzo, and N. Fornengo, Constraints on the coupling between dark energy and dark matter from CMB data, J. Cosmol. Astropart. Phys. 04 (2016) 014.

[13] M. Lucca, Dark energy–dark matter interactions as a solution to the S8 tension, Phys. Dark Univ. **34**, 100899 (2021).

[14] V. Poulin, J. L. Bernal, E. D. Kovetz, and M. Kamionkowski, Sigma-8 tension is a drag, Phys. Rev. D **107**, 123538 (2023).

[15] K. Enqvist, S. Nadathur, T. Sekiguchi, and T. Takahashi, Decaying dark matter and the tension in σ_8, J. Cosmol. Astropart. Phys. 09 (2015) 067..

[16] K. L. Pandey, T. Karwal, and S. Das, Alleviating the H_0 and σ_8 anomalies with a decaying dark matter model, J. Cosmol. Astropart. Phys. 07 (2020) 026.

[17] G. F. Abellán, R. Murgia, V. Poulin, and J. Lavalle, Implications of the S_8 tension for decaying dark matter with warm decay products, Phys. Rev. D **105**, 063525 (2022).

[18] G. F. Abellán, R. Murgia, and V. Poulin, Linear cosmological constraints on two-body decaying dark matter scenarios and the S8 tension, Phys. Rev. D **104**, 123533 (2021).

[19] T. Simon, G. F. Abellán, P. Du, V. Poulin, and Y. Tsai, Constraining decaying dark matter with BOSS data and the effective field theory of large-scale structures, Phys. Rev. D **106**, 023516 (2022).

[20] A. Amon and G. Efstathiou, A non-linear solution to the S_8 tension? Mon. Not. R. Astron. Soc. **516**, 5355 (2022).

[21] G. Aricò, R. E. Angulo, M. Zennaro, S. Contreras, A. Chen, and C. Hernández-Monteagudo, DES Y3 cosmic shear down to small scales: Constraints on cosmology and baryons, Astron. Astrophys. **678**, A109 (2023).

[22] S. Chabanier, M. Millea, and N. Palanque-Delabrouille, Matter power spectrum: From Lyα forest to CMB scales, Mon. Not. R. Astron. Soc. **489**, 2247 (2019).

[23] Z. Lukić, C. W. Stark, P. Nugent, M. White, A. A. Meiksin, and A. Almgren, The Lyman-α forest in optically thin hydrodynamical simulations, Mon. Not. R. Astron. Soc. **446**, 3697 (2015).

[24] B. W. Lyke *et al.*, The sloan digital sky survey quasar catalog: Sixteenth data release, Astrophys. J. Suppl. **250**, 8 (2020).

[25] S. Chabanier *et al.*, The one-dimensional power spectrum from the SDSS DR14 Lyα forests, J. Cosmol. Astropart. Phys. 07 (2019) 017.

[26] A. Borde, N. Palanque-Delabrouille, G. Rossi, M. Viel, J. S. Bolton, C. Yèche, J.-M. LeGoff, and J. Rich, New approach for precise computation of Lyman-α forest power spectrum with hydrodynamical simulations, J. Cosmol. Astropart. Phys. 07 (2014) 005.

[27] N. Palanque-Delabrouille, C. Yèche, N. Schöneberg, J. Lesgourgues, M. Walther, S. Chabanier, and E. Armengaud, Hints, neutrino bounds and WDM constraints from SDSS DR14 Lyman-α and Planck full-survey data, J. Cosmol. Astropart. Phys. 04 (2020) 038.

[28] C. Pedersen, A. Font-Ribera, K. K. Rogers, P. McDonald, H. V. Peiris, A. Pontzen, and A. Slosar, An emulator for the Lyman-α forest in beyond-ΛCDM cosmologies, J. Cosmol. Astropart. Phys. 05 (2021) 033.

[29] C. Pedersen, A. Font-Ribera, T. D. Kitching, P. McDonald, S. Bird, A. Slosar, K. K. Rogers, and A. Pontzen, Massive neutrinos and degeneracies in Lyman-alpha forest simulations, J. Cosmol. Astropart. Phys. 04 (2020) 025.

[30] C. Pedersen, A. Font-Ribera, and N. Y. Gnedin, Compressing the cosmological information in one-dimensional correlations of the Lyα forest, Astrophys. J. **944**, 223 (2023).

[31] P. McDonald, J. Miralda-Escudé, M. Rauch, W. L. W. Sargent, T. A. Barlow, R. Cen, and J. P. Ostriker, The observed probability distribution function, power spectrum, and correlation function of the transmitted flux in the Ly-alpha forest*, Astrophys. J. **543**, 1 (2000).

[32] See Supplemental Material at http://link.aps.org/supplemental/10.1103/PhysRevResearch.7.L012018 for details of the likelihoods, analysis details and full sets of marginalized posteriors.

[33] S. Goldstein, J. C. Hill, V. Iršič, and B. D. Sherwin, Canonical Hubble-tension-resolving early dark energy cosmologies are inconsistent with the Lyman-α forest, Phys. Rev. Lett. **131**, 201001 (2023).

[34] S. Alam *et al.* (BOSS Collaboration), The clustering of galaxies in the completed SDSS-III Baryon Oscillation Spectroscopic Survey: Cosmological analysis of the DR12 galaxy sample, Mon. Not. R. Astron. Soc. **470**, 2617 (2017).

[35] F. Beutler, C. Blake, M. Colless, D. H. Jones, L. Staveley-Smith, L. Campbell, Q. Parker, W. Saunders, and F. Watson, The 6dF Galaxy Survey: Baryon acoustic oscillations and the local Hubble constant, Mon. Not. R. Astron. Soc. **416**, 3017 (2011).

[36] A. J. Ross, L. Samushia, C. Howlett, W. J. Percival, A. Burden, and M. Manera, The clustering of the SDSS DR7 main Galaxy sample–I. A 4 per cent distance measure at $z = 0.15$, Mon. Not. R. Astron. Soc. **449**, 835 (2015).

[37] V. Poulin, T. L. Smith, D. Grin, T. Karwal, and M. Kamionkowski, Cosmological implications of ultralight axion-like fields, Phys. Rev. D **98**, 083525 (2018).

[38] T. L. Smith, V. Poulin, and M. A. Amin, Oscillating scalar fields and the Hubble tension: A resolution with novel signatures, Phys. Rev. D **101**, 063523 (2020).

[39] M. Raveri and C. Doux, Non-Gaussian estimates of tensions in cosmological parameters, Phys. Rev. D **104**, 043504 (2021).

[40] K. K. Rogers, S. Bird, H. V. Peiris, A. Pontzen, A. Font-Ribera, and B. Leistedt, Simulating the effect of high column density absorbers on the one-dimensional Lyman α forest flux power spectrum, Mon. Not. R. Astron. Soc. **474**, 3032 (2018).

[41] K. K. Rogers, S. Bird, H. V. Peiris, A. Pontzen, A. Font-Ribera, and B. Leistedt, Correlations in the three-dimensional Lyman-alpha forest contaminated by high column density absorbers, Mon. Not. R. Astron. Soc. **476**, 3716 (2018).

[42] M. Vogelsberger, S. Genel, V. Springel, P. Torrey, D. Sijacki, D. Xu, G. F. Snyder, S. Bird, D. Nelson, and L. Hernquist, Properties of galaxies reproduced by a hydrodynamic simulation, Nature (London) **509**, 177 (2014).

[43] S. Bird, M. Vogelsberger, M. Haehnelt, D. Sijacki, S. Genel, P. Torrey, V. Springel, and L. Hernquist, Damped Lyman-α absorbers as a probe of stellar feedback, Mon. Not. R. Astron. Soc. **445**, 2313 (2014).

[44] S. Chabanier, F. Bournaud, Y. Dubois, N. Palanque-Delabrouille, C. Yèche, E. Armengaud, S. Peirani, and R. Beckmann, The impact of AGN feedback on the 1D power spectra from the Ly-α forest using the Horizon-AGN suite of simulations, Mon. Not. R. Astron. Soc. **495**, 1825 (2020).

[45] Y. Dubois, S. Peirani, C. Pichon, J. Devriendt, R. Gavazzi, C. Welker, and M. Volonteri, The Horizon-AGN simulation: Morphological diversity of galaxies promoted by AGN feedback, Mon. Not. R. Astron. Soc. **463**, 3948 (2016).

[46] P. F. Hopkins *et al.*, FIRE-2 simulations: Physics versus numerics in galaxy formation, Mon. Not. R. Astron. Soc. **480**, 800 (2018).

[47] M. A. Fernandez, S. Bird, and M.-F. Ho, Cosmological constraints from the eBOSS Lyman-α Forest using the PRIYA simulations, J. Cosmol. Astropart. Phys. 07 (2024) 029.

[48] S. Bird, M. Fernandez, M.-F. Ho, M. Qezlou, R. Monadi, Y. Ni, N. Chen, R. Croft, and T. Di Matteo, PRIYA: A new suite of Lyman-α forest simulations for cosmology, J. Cosmol. Astropart. Phys. 10 (2023) 037.

[49] P. Gaikwad, R. Srianand, M. G. Haehnelt, and T. R. Choudhury, A consistent and robust measurement of the thermal state of the

IGM at $2 \leqslant z \leqslant 4$ from a large sample of Ly α forest spectra: Evidence for late and rapid He II reionization, Mon. Not. R. Astron. Soc. **506**, 4389 (2021).

[50] M. Walther, N. Schöneberg, S. Chabanier, E. Armengaud, J. Sexton, C. Yèche, J. Lesgourgues, M. R. Mosbech, C. Ravoux, N. Palanque-Delabrouille, and Z. Lukić, Emulating the Lyman-alpha forest 1D power spectrum from cosmological simulations: New models and constraints from the eBOSS measurement, arXiv:2412.05372.

[51] C. Ramirez-Perez *et al.* (DESI Collaboration), The Lyman-α forest catalog from the Dark Energy Spectroscopic Instrument Early Data Release, arXiv:2306.06312.

[52] A. Abate *et al.* (LSST Dark Energy Science Collaboration), Large synoptic survey telescope: Dark energy science collaboration, arXiv:1211.0310.

[53] P. Ade *et al.* (Simons Observatory Collaboration), The Simons Observatory: Science goals and forecasts, J. Cosmol. Astropart. Phys. 02 (2019) 056.

[54] M. Archidiacono, D. C. Hooper, R. Murgia, S. Bohr, J. Lesgourgues, and M. Viel, Constraining dark matter-dark radiation interactions with CMB, BAO, and Lyman-α, J. Cosmol. Astropart. Phys. 10 (2019) 055.

[55] E. Boera, G. D. Becker, J. S. Bolton, and F. Nasir, Revealing reionization with the thermal history of the intergalactic medium: New constraints from the Lyα flux power spectrum, Astrophys. J. **872**, 101 (2019).

[56] A. Day, D. Tytler, and B. Kambalur, Power spectrum of the flux in the Lyman-alpha forest from high-resolution spectra of 87 QSOs, Mon. Not. R. Astron. Soc. **489**, 2536 (2019).

[57] N. G. Karaçaylı *et al.*, Optimal 1D Ly α forest power spectrum estimation–II. KODIAQ, SQUAD, and XQ-100, Mon. Not. R. Astron. Soc. **509**, 2842 (2021).

[58] V. Iršič *et al.*, The Lyman α forest power spectrum from the XQ-100 Legacy Survey, Mon. Not. R. Astron. Soc. **466**, 4332 (2017).

[59] K. K. Rogers and H. V. Peiris, Strong bound on canonical ultralight axion dark matter from the Lyman-alpha forest, Phys. Rev. Lett. **126**, 071302 (2021).

[60] K. K. Rogers, C. Dvorkin, and H. V. Peiris, Limits on the light dark matter–proton cross section from cosmic large-scale structure, Phys. Rev. Lett. **128**, 171301 (2022).

[61] K. K. Rogers and H. V. Peiris, General framework for cosmological dark matter bounds using N-body simulations, Phys. Rev. D **103**, 043526 (2021).

[62] E. O. Nadler *et al.* (DES Collaboration), Milky way satellite census. III. Constraints on dark matter properties from observations of Milky Way satellite galaxies, Phys. Rev. Lett. **126**, 091101 (2021).

[63] W. Enzi *et al.*, Joint constraints on thermal relic dark matter from strong gravitational lensing, the Ly α forest, and Milky Way satellites, Mon. Not. R. Astron. Soc. **506**, 5848 (2021).

[64] N. Banik, J. Bovy, G. Bertone, D. Erkal, and T. J. L. de Boer, Novel constraints on the particle nature of dark matter from stellar streams, J. Cosmol. Astropart. Phys. 10 (2021) 043.

[65] D. C. Hooper and M. Lucca, Hints of dark matter-neutrino interactions in Lyman-α data, Phys. Rev. D **105**, 103504 (2022).

[66] D. C. Hooper, N. Schöneberg, R. Murgia, M. Archidiacono, J. Lesgourgues, and M. Viel, One likelihood to bind them all: Lyman-α constraints on non-standard dark matter, J. Cosmol. Astropart. Phys. 10 (2022) 032.

[67] M. Esposito, V. Iršič, M. Costanzi, S. Borgani, A. Saro, and M. Viel, Weighing cosmic structures with clusters of galaxies and the intergalactic medium, Mon. Not. R. Astron. Soc. **515**, 857 (2022).

[68] L. E. Bleem, B. Stalder, T. de Haan, K. A. Aird, S. W. Allen, D. E. Applegate, M. L. N. Ashby, M. Bautz, M. Bayliss, B. A. Benson, S. Bocquet, M. Brodwin, J. E. Carlstrom, C. L. Chang, I. Chiu, H. M. Cho, A. Clocchiatti, T. M. Crawford, A. T. Crites, S. Desai *et al.*, Galaxy clusters discovered via the Sunyaev–Zel'dovich effect in the 2500-square-degree SPT-SZ survey, Astrophys. J. Suppl. Ser. **216**, 27 (2015).